115 (1968).
[20]C. R. Hall and P. B. Hirsch, Proc. Roy. Soc. (London) A286, 158 (1965).
[21]H. Yoshioka and Y. Kainuma, J. Phys. Soc. Japan Suppl. 17, 134 (1962).

PHYSICAL REVIEW B VOLUME 3, NUMBER 11 1 JUNE 1971

Nuclear Magnetic Resonance and Relaxation in the "Liquid Semiconductors" In_2Te_3, Ga_2Te_3, and Sb_2Te_3

William W. Warren, Jr.
Bell Telephone Laboratories, Murray Hill, New Jersey 07974
(Received 20 January 1971)

Measurements of the Knight shifts of In^{115}, Ga^{69}, Ga^{71}, Sb^{121}, Sb^{123}, and Te^{125} in solid and liquid In_2Te_3, Ga_2Te_3, and Sb_2Te_3 are reported for temperatures ranging from roughly 150 K below the melting points to 1400–1500 K. Measurements of the nuclear spin-spin relaxation rates of In^{115}, Ga^{69}, Ga^{71}, Sb^{121}, and Sb^{123} are reported for the liquids from the melting points to 1400–1500 K. The data are discussed in terms of various theoretical models for the electronic structure of liquid semiconductors. It is shown that nuclear relaxation-rate measurements provide a means for characterization of the microscopic electronic transport mechanism. In the case of In_2Te_3 and Ga_2Te_3 an unusual enhancement of the nuclear relaxation rate relative to the predicted Korringa rate is shown to be consistent with the existence of localized electronic states at the Fermi level. Sb_2Te_3, on the other hand, exhibits no appreciable enhancement and is characterized as a metallic liquid. A general scheme is proposed for classification of the electron dynamics in electronically conducting liquids by the correlation of the nuclear relaxation rate and the dc conductivity.

I. INTRODUCTION

A number of electronically conducting liquids have been described as "liquid semiconductors" because their transport properties are reminiscent of those found for ordinary crystalline semiconductors. Although the properties of these liquids are widely varied, some general characteristics may be said to be typical of the group.[1] For example, most of the known liquid semiconductors are binary alloys or compounds consisting of a metallic component and a chalcogenide (O, S, Te, or Se) and they are invariably semiconducting in the solid phase. The liquids exhibit electrical conductivities σ less than about 10^3 $(\Omega\,\mathrm{cm})^{-1}$, and the conductivity increases with increasing temperature. In some cases, the temperature dependence of σ for the liquid is essentially a continuation of that of the corresponding solid, while in others (notably those with higher values of σ) the temperature variation changes markedly at the melting point T_m. The Hall coefficients have been measured for a few liquid semiconductors and have been found to be negative and significantly larger than free-electron values calculated for the total number of valence electrons. The Seebeck coefficients exhibit complex behavior in that they may be either positive or negative and, in fact, they often change sign with variations in temperature or alloy composition.

Theoretical understanding of the properties of liquid semiconductors in terms of their electronic structure is still at an early stage. The transport properties show clearly that these liquids are very different from ordinary liquid metals and metallic "molten semiconductors," such as Si or InSb. On the other hand, it is by no means evident that conventional semiconductor concepts derived for crystals may be extended to liquids without major modifications. This situation has led to new and, in some respects, conflicting speculations concerning the electronic structure of liquid and amorphous-solid semiconductors. The models differ particularly in their assumptions concerning the localized nature of the electronic eigenstates and details of electronic transport. These assumptions concern phenomena which are microscopic in that they occur over distances comparable to the interatomic spacing and, unfortunately, they are difficult to test directly by measurements of bulk transport properties at elevated temperatures.

In this paper we describe the application of nuclear magnetic resonance (NMR) to the study of liquid semiconductors. We show that the sensitivity of NMR experiments to details of the microscopic electronic and molecular dynamics yields important information not available from transport measurements. Specifically, we will report and discuss measurements of the Knight shifts and nuclear relaxation rates for In^{115} in liquid In_2Te_3, Ga^{69} and Ga^{71} in liquid Ga_2Te_3, and Sb^{121} and Sb^{123} in liquid

Sb_2Te_3.[2] The Knight shifts for Te^{125} in all three liquids and the Knight shifts for all the above nuclei in the solids near the melting points are described also.

The organization of the paper is as follows. In Sec. II we discuss the principal theoretical models and the relationship of NMR data to the important theoretical parameters. Sections III and IV contain, respectively, details of the experimental technique and experimental results for In_2Te_3, Ga_2Te_3, and Sb_2Te_3. The experimental results are discussed in Sec. V and, in particular, the data are related to the theoretical models and to a transport property (dc conductivity). Finally, the principal conclusions of the work are summarized in Sec. VI.

II. THEORY

A. Models for Electronic Structure of Liquid Semiconductors

1. *Conventional Semiconductor Theory*

Early attempts[3] to account for the properties of liquid semiconductors were made, quite naturally, within the framework of conventional semiconductor theory as it applies to crystalline semiconductors. Thus, it was supposed, the electronic states exhibit a band structure with a density of states consisting of the usual valence and conduction bands separated by an energy gap of width E_{gap} [Fig. 1(a)]. The nature of the conductivity might be n type or p type, extrinsic or intrinsic, depending on the values of E_{gap}, temperature, and impurity concentrations.

These conventional concepts were used extensively by Cutler and co-workers in a comprehensive series of papers[4–8] dealing with the transport properties of liquid Tl-Te alloys. The conductivity of these alloys shows a sharp minimum at a concentration close to Tl_2Te and the sign of the Seebeck coefficient α changes from positive to negative as the Tl concentration is increased through Tl_2Te. Cutler *et al.* assumed that the sign of the majority carriers corresponds to the sign of the Seebeck coefficient and thus inferred that near Tl_2Te excess Tl or Te atoms act as donors or acceptors, respectively. The persistent negative sign of the Hall coefficient in the so-called p type ($\alpha > 0$) alloys remained to be explained on independent grounds.

2. *Pseudogap with Localized States*

This model has been brought to its present state in a series of papers by Mott[9–16] although some of its features date from earlier work of Anderson,[17] Gubanov,[18] and Banyai.[19] The model is derived from consideration of the effects of disorder on the electronic structure of the crystalline system and it has been applied to both liquid and amorphous-solid semiconductors.[16,20,21] There are two principal features, illustrated in Fig. 1(b), with which we shall be mainly concerned. First, in the presence of disorder due to fluctuations in the local atomic arrangement (structural disorder), the valence and conduction band edges become smeared and acquire "tails" which extend well into the crystalline band gap. In liquid semiconductors the tails may overlap to the extent that the gap is replaced by a "pseudogap" or minimum in the density of states. The second and most distinctive feature of the model is derived from the observation that those states whose energies lie in or near the original gap are strongly scattered by the lattice and thus are extremely sensitive to the presence of disorder. Under suitable conditions, it is argued, disorder leads to modification of the character of the electronic eigenstates from the extended (Bloch) states of the ordered system to localized states in the liquid or amorphous system. Since the states in the pseudogap are taken to be most sensitive to disorder, one might expect to find a band of such localized states in the pseudogap which connects valence and conduction bands containing extended states. Within the band of localized states, electronic transport requires phonon assistance whereas in the nonlocalized region electrons scatter between nearly-

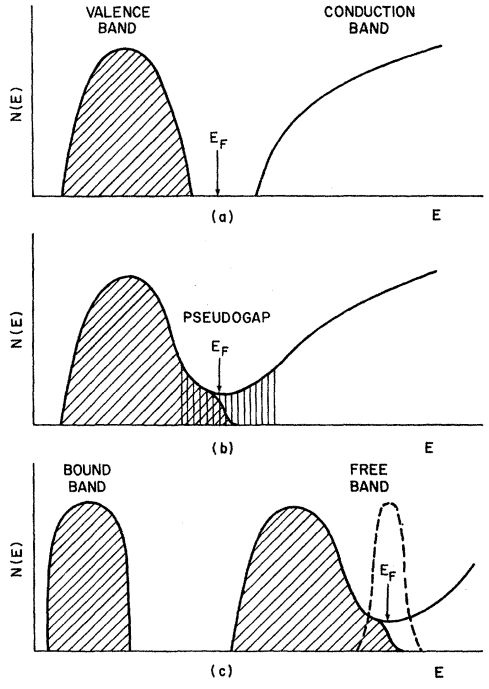

FIG. 1. Density of states $N(E)$ for a liquid semiconductor as a function of energy E according to various models: (a) conventional semiconductor model; (b) pseudogap model; (c) pseudobinary alloy model. Diagonal shading denotes occupied energy levels. Vertical shading (b) denotes localized states. Broken line (c) describes energy dependence of scattering cross section.

free-electron (NFE) states as in liquid metals. The localized states are easily distinguished in the formal sense since they make vanishing contributions to the dc electrical conductivity as the temperature approaches absolute zero.

The conditions for occurrence of localized states in a pseudogap have been discussed in some detail by Mott.[12] We mention here two points which are particularly relevant to the discussion of our NMR results. First, Mott has argued that localization will not normally occur in liquids if the electronic wave functions are s-like *on all atoms*. However, if the wave functions are p-like (or d-like, etc.) on some of the atoms, then the increased sensitivity to disorder provided by the directional character of the bonds makes localization much more likely. The second point is that the occurrence of localized states depends on the depth of the pseudogap. That is, states will begin to become localized when the interaction with the ions is sufficiently strong to lower the density of states in the pseudogap below some critical value. Mott[12] has extended Anderson's criterion[17] for localization in the presence of a randomly varying crystalline potential (cellular disorder) and has argued that states of a given energy E will localize when

$$g \equiv N(E)/N(E)_{fe} \leq 1/3.5 = 0.285 , \tag{1}$$

where $N(E)$ and $N(E)_{fe}$ are, respectively, the actual and free-electron density of states.

3. *Pseudobinary Alloy*

This model has been developed from consideration of the transport properties of binary liquid alloy systems by Enderby and Simmons[22] and Enderby and Collings.[23] These authors have suggested that the sharp minima of the conductivities of Tl-Te and Mg-Bi near Tl_2Te and Mg_3Bi_2 result from formation of molecular bound states of these stoichiometric compositions. Thus, near stoichiometry the liquid is regarded as "alloy" consisting of a molecular component (e.g., Mg_3Bi_2) and a metallic component (e.g., Mg or Bi). The density of states, shown in Fig. 1(c), consists of a filled "bound band" separated by a real energy gap from a NFE "free band." The number of carriers is determined by the number of electrons in the free band which depends, in turn, on the alloy composition.

The pseudobinary alloy concept contrasts with the conventional semiconductor model in that electrons are the current carriers at all compositions whereas the conventional model permits both n- and p-type conduction. This distinction rests on the assumption in the pseudobinary alloy model that the Hall coefficient rather than the Seebeck coefficient provides the true indication of the sign of the carriers. In order to explain the rapid variation and sign change of α near stoichiometry, Enderby and co-workers postulated the existence of a strongly energy-dependent scattering or "virtual bound state" for electrons near the Fermi level. Their argument is based on the following formula for α[24]:

$$\alpha = \frac{\pi^3}{3}\frac{k^2 T}{e}\left(\frac{\partial \ln\sigma(E)}{\partial E}\right)_{E_F} , \tag{2}$$

where $\sigma(E)$ is the contribution to the conductivity from electrons with energy E. If the scattering cross section is sharply peaked near E_F for the stoichiometric alloy [Fig. 1(c)], then Eq. (2) predicts that α must change sign as the variation of composition sweeps E_F through the region of the virtual bound state. From consideration of the required energy dependence of $\sigma(E)$ Enderby and coworkers estimated the widths of the virtual bound states to be 0.2 eV for Tl_2Te and 0.6 eV for Mg_3Bi_2. The source of the energy-dependent scattering was taken to be scattering from excess Tl or Te atoms in Ref. 22 while it is suggested in Ref. 23 that the virtual bound state results from scattering from molecular groups such as Mg_3Bi_2 in Mg-Bi. The essential features of the model are, however, quite similar in either case.

The present model differs from the pseudogap model mainly in that the conduction-electron states are extended (i.e., metallic) at all temperatures and compositions and do not become localized. Thus, according to Enderby and Simmons, the conductivity is given by an equation of the standard type valid for metals[25]

$$\frac{1}{\sigma} = \frac{m v_F}{n e^2}\left(\frac{1}{\Lambda_0} + \frac{1}{\Lambda_1}\right) , \tag{3}$$

where v_F is the Fermi velocity, n is the electron concentration, and Λ_0 and Λ_1 are the mean free paths for scattering by the molecular component and the metallic component, respectively. For Tl-Te, Λ_0 and Λ_1 are not less than about one interatomic distance (about 2 Å). The essential distinction to be made here is that even in the presence of a virtual bound state the electron dynamics are of an essentially metallic character and are described in terms of the scattering of electrons moving at the Fermi velocity with a well-defined mean free path.

B. Interpretation of NMR Experiments in Liquid Semiconductors

The two principal quantities to be determined from NMR studies of liquid semiconductors are the Knight shift $\mathcal{K}$ and the nuclear spin-lattice relaxation rate $1/T_1$. As is also true for solid and liquid metals, the Knight shift and spin-lattice relaxation are consequences of the static and dynamic parts, respectively, of magnetic hyperfine interactions with the conduction electrons. In addition, if the

nuclei possess electric quadrupole moments, there may be observable contributions to spin-lattice relaxation from dynamic quadrupolar interactions produced by ionic and molecular motions. There are no quadrupolar shifts because static quadrupolar interactions are averaged to zero by the rapid internal motions of the liquid. In this section we discuss the interpretation of measurements of $\mathcal{K}$ and $1/T_1$ in liquid semiconductors with emphasis on the connection between these parameters and the important features of the theoretical models.

1. *Knight Shift*

In this paper we are concerned mainly with situations in which the conduction electrons exhibit predominantly s character at the nuclear site of interest. In such a case the dominant term in the magnetic hyperfine interaction is the Fermi contact interaction whose Hamiltonian is

$$\mathcal{H}_c = (\tfrac{8}{3}\pi)\gamma_n\gamma_e\hbar^2\vec{I}\cdot\vec{S}\delta(\vec{r}) , \tag{4}$$

where γ_n and γ_e are, respectively, the nuclear and electronic gyromagnetic ratios, $\vec{I}$ and $\vec{S}$ are the nuclear and electronic spin operators, and $\vec{r}$ is the electron coordinate. Application of time-independent perturbation theory and performance of a thermal average over the electron system then leads directly to the following expression for the Knight shift[26]:

$$\mathcal{K} = \frac{\Delta H}{H_0} = \frac{4\pi}{3}\frac{\gamma_e\hbar}{H_0}\int_0^\infty dE\,|\psi_E(0)|^2 N(E)[f(E,+) - f(E,-)] . \tag{5}$$

In Eq. (5) H_0 is the applied magnetic field, $|\psi_E(0)|^2$ is the probability density at the nucleus for electrons of energy E, $N(E)$ is the density of states per atom for a single direction of electron spin, and the Fermi functions $f(E,\pm)$ are given by

$$f(E,\pm) = \{\exp[(E \mp \tfrac{1}{2}\gamma_e\hbar H_0 - E_F)/kT] + 1\}^{-1} . \tag{6}$$

For a conventional intrinsic semiconductor [Fig. 1(a)], $\mathcal{K}$ is obtained by evaluating the integral in Eq. (5) over the detailed form of $N(E)$ determined by the band structure. Considerable simplification is achieved in situations such as those represented by Figs. 1(b) and 1(c). In these cases the electron system is degenerate and variation of $N(E)$ is negligible over an energy interval of width kT near E_F. The approximation

$$f(E,+) - f(E,-) \simeq \gamma_e\hbar H_0\delta(E - E_F) \tag{7}$$

then leads to the familiar expression, also valid for metals,

$$\mathcal{K} = \tfrac{4}{3}\pi(\gamma_e\hbar)^2\langle|\psi(0)|^2\rangle_F N(E_F) , \tag{8}$$

where $\langle|\psi(0)|^2\rangle_F$ represents the s-electron probability amplitude at the nucleus averaged over all states at the Fermi level.

In principle, Eq. (8) can be used to determine $N(E_F)$ from experimental values of $\mathcal{K}$. Unfortunately, this procedure is subject to several uncertainties which rather severely limit its accuracy. In the first place, of course, is the fact that $\langle|\psi(0)|^2\rangle_F$ is not generally known with precision. Although it is possible to determine $\langle|\psi(0)|^2\rangle_F$ from electron-spin-resonance data, this has been done for only a few special systems such as some of the alkali metals[27,28] and the III-V semiconductor InSb.[29] More generally one can make use of atomic values of $|\psi_A(0)|^2$ obtained from optical hyperfine structure and correct these with calculated or otherwise estimated values of the "penetration factor"[30]

$$\xi \equiv \langle|\psi(0)|^2\rangle_F / |\psi_A(0)|^2 . \tag{9}$$

In Li and Na the values of ξ are known[27,28] to be 0.44 and 0.60, respectively, and various calculations and estimates yield similar values for a number of other metals.[30,31] For crystalline InSb, direct measurement[29] of $|\psi(0)|^2_{\mathrm{In}}$ yielded a value 0.62 for ξ.

Another important correction to Eq. (8) results from neglect of electron-electron interactions. The exchange and correlation effects in metals are known[27,32] to produce appreciable enhancements of $\mathcal{K}$ relative to the value given by Eq. (8). The enhancements in alkali metals, for example, lie in the range 1.7–2.0. Thus, in this case, the effects of electron-electron interactions and the penetration factor are roughly equal in magnitude but have opposite signs. In the absence of specific data for either correction in liquid semiconductors the most straightforward approach is simply to neglect both these effects and employ Eq. (8) with values of $\langle|\psi(0)|^2\rangle_F$ equal to the optical hyperfine coupling. This procedure should suffice to yield estimates of $N(E_F)$ accurate to within about 30%.

An alternative procedure, possible in some special cases, consists of comparing the value of $\mathcal{K}$ in the liquid semiconductor with the value of $\mathcal{K}$ for the same nucleus in a system of similar composition for which $N(E_F)$ is known. Thus, for example, if there exists a temperature or composition range for which the system of interest is a sufficiently good metal so that $N(E_F)$ may be assumed to be close to the free-electron value, we may take

$$g = N(E_F)/N(E_F)_{fe} \simeq \mathcal{K}\,(\text{liquid semiconductor})/\mathcal{K}(\text{metal}). \tag{10}$$

In using this method it is assumed that ξ and the electron-electron effects are the same in the metal and liquid semiconductor and that the degree of s

character is roughly the same in both systems.

Finally, we reemphasize that Eq. (8) describes only the contribution to $\mathcal{K}$ from s-electron contact interactions. If the wave functions contain a large fraction of p character at the nuclear site in question, additional contributions to $\mathcal{K}$ may be expected from core polarization and orbital interactions. Since these p-electron hyperfine fields are normally about an order of magnitude smaller than s-electron fields, the use of Eq. (8) in the presence of appreciable p character would lead to an underestimate of $N(E_F)$.

2. *Spin-Lattice Relaxation*

It is convenient to discuss spin-lattice relaxation in liquid semiconductors in terms of the time correlation functions for the interactions responsible for relaxation. For a system of nuclear spins perturbed by an interaction $\mathcal{H}'(t)$ which is a random function of time, the probability for a nuclear spin to undergo a transition from a Zeeman state m to a state $m+\mu$ is given by the standard formula[33]

$$W_{m,m+\mu} = \hbar^{-2} \int_{-\infty}^{\infty} dt\, e^{i\mu\omega_0 t} \{\langle m|\mathcal{H}'(t)|m+\mu\rangle \times \langle m+\mu|\mathcal{H}'(0)|m\rangle\}, \quad (11)$$

where ω_0 is the nuclear Larmor frequency and the curly brackets denote an ensemble average. A common approximation is to let

$$\{\langle m|\mathcal{H}'(t)|m+\mu\rangle\langle m+\mu|\mathcal{H}'(0)|m\rangle\} = \{|\langle m|\mathcal{H}'|m+\mu\rangle|^2\} e^{-|t|/\tau}, \quad (12)$$

where τ is an appropriate correlation time for the interaction. Upon substitution into Eq. (11), Eq. (12) leads to the following general form for the transition probability:

$$W_{m,m+\mu} = \frac{1}{\hbar^2} \{|\langle m|\mathcal{H}'|m+\mu\rangle|^2\} \frac{2\tau}{1+(\mu\omega_0\tau)^2}. \quad (13)$$

For the purposes of the present paper we need consider only the short correlation time limit ($\omega_0\tau \ll 1$) in which the nuclear magnetization may be shown[34] to approach equilibrium with a single time constant T_1, where

$$\frac{1}{T_1} \equiv R = \frac{4}{\hbar^2} \{|\langle m|\mathcal{H}'|m+\mu\rangle|^2\}\tau. \quad (14)$$

We emphasize that the exponential form [Eq. (12)] for the correlation function is introduced *ad hoc* without further justification. Nevertheless it describes the essential physics encountered in many physical systems and we shall assume that numerical results obtained from the use of Eq. (14) are at least semiquantitatively correct.

The interactions $\mathcal{H}'$ causing relaxation may be classed as either of two types depending on whether they involve coupling between the nuclear dipole moment and perturbing magnetic fields ("magnetic relaxation") or coupling between the nuclear electric quadrupole moment and fluctuating electric field gradients ("quadrupolar relaxation"). In general the observed rate R may contain contributions from both kinds of interaction and it is not possible to separate these unambiguously. However, if measurements of $1/T_1$ can be made for two isotopes of the same atomic species (e.g., Ga^{69} and Ga^{71}), direct decomposition may be accomplished. Thus, given experimental values for the relaxation rates R^A and R^B for two isotopes A and B at a common temperature, it is straightforward to compute the magnetic and quadrupolar contributions R_M^A, R_Q^A, R_M^B, and R_Q^B according to the following formulas[35]:

$$R_M^A = \frac{R^A - \alpha_Q R^B}{1-\alpha_Q/\alpha_M}, \quad (15a)$$

$$R_Q^A = \frac{R^A - \alpha_M R^B}{1-\alpha_M/\alpha_Q}, \quad (15b)$$

$$R_M^B = R_M^A/\alpha_M, \quad (15c)$$

$$R_Q^B = R_Q^A/\alpha_Q, \quad (15d)$$

where the parameters α_Q and α_M are given in terms of the gyromagnetic ratios γ, nuclear spins I, and quadrupole moments Q by

$$\alpha_Q = f(I_A)Q_A^2/f(I_B)Q_B^2, \quad (16a)$$

$$\alpha_M = (\gamma_A/\gamma_B)^2, \quad (16b)$$

$$f(I) = (2I+3)/I^2(2I-1). \quad (16c)$$

a. Magnetic relaxation. The dominant magnetic relaxation process in metals and degenerate semiconductors is usually the Korringa process[36] in which nuclei couple to the spins of s-like conduction electrons through the Fermi contact interaction [Eq. (4)]. If electron-electron interactions are neglected and the electrons are considered to occupy plane-wave or Bloch states, the relaxation rate is given by the familiar formula

$$R_M = \tfrac{64}{9}\pi^3\hbar^3\gamma_e^2\gamma_n^2 kT[N(E_F)]^2\langle|\psi(0)|^2\rangle_F^2, \quad (17)$$

where T is the temperature. This relaxation rate may be expressed in terms of the Knight shift by direct substitution of $\langle|\psi(0)|^2\rangle_F N(E_F)$ from Eq. (8) to yield the Korringa relation[36]

$$R_M = 4\pi\gamma_n^2 kT\mathcal{K}^2/\gamma_e^2\hbar. \quad (18)$$

While Eq. (18) is subject to modification by inclusion of the effects of p electrons and electron-electron interaction,[37,38] it remains an extremely useful approximation because its parameters are available

from independent experiments. In liquid metals the deviations from Eq. (18) lie mostly in the range $\pm 30\%$.[35,39]

The Korringa relaxation process is ordinarily independent of the details of electron transport. Thus in metals and crystalline semiconductors there is no direct connection between R_M and, say, the electron mean free path Λ. The reason is easily seen if we express R_M in terms of a correlation time as in Eq. (14). In this case the appropriate correlation time is the time τ_e during which an electron interacts with a particular nucleus. For NFE, τ_e is roughly the time required for an electron traveling at the Fermi velocity to traverse one nearest-neighbor distance a and, so long as $\Lambda > a$, τ_e is independent of Λ. For NFE the Fermi velocity is related to the density of states by[40]

$$v_F = 2a/z\hbar N(E_F) , \tag{19}$$

where z is the number of electrons per atom. Hence,

$$\tau_e \simeq a/v_F \simeq \hbar N(E_F) , \quad \Lambda > a . \tag{20}$$

We now consider the case in which electron transport cannot be described by a mean free path at least as great as the interatomic spacing. Although no detailed theory of nuclear relaxation yet exists for this regime of very strong scattering we can use the correlation-time formalism to derive an approximate analog of the Korringa relation. Thus, from Eq. (14),

$$R_M \simeq (4/\hbar^2)\{|\langle -\tfrac{1}{2}|\mathcal{H}_c|\tfrac{1}{2}\rangle|^2\}\tau_e , \tag{21}$$

where $\mathcal{H}_c$ is given by Eq. (4) and τ_e now has the significance of the lifetime for "residence" of an electron on a nuclear site. The coupling strength is, approximately,

$$\{|\langle -\tfrac{1}{2}|\mathcal{H}_c|\tfrac{1}{2}\rangle|^2\} \simeq (\tfrac{8}{3}\pi)^2\gamma_n^2\gamma_e^2\hbar^4\langle|\psi(0)|^2\rangle_F^2 N(E_F)kT \tag{22}$$

in which the factor $N(E_F)kT$ is introduced to account for the effect of energy conservation which restricts participation in the relaxation process to electrons whose energies lie within an interval of width kT at the Fermi level. Expressing $\langle|\psi(0)|^2\rangle_F^2$ in terms of $\mathcal{K}^2$ by means of Eq. (8) we obtain

$$R_M = 16\gamma_n^2\mathcal{K}^2 kT\tau_e/\gamma_e^2\hbar^2 N(E_F) . \tag{23}$$

In the long mean-free-path limit, τ_e is given by Eq. (20) and, to within a factor $4/\pi$, Eq. (23) reduces to the standard Korringa form given by Eq. (18).

The crucial feature of Eq. (23) is that it predicts an enhancement of R_M relative to the prediction of Eq. (18) if the electrons remain in the vicinity of the nucleus for average times longer than $\hbar N(E_F)$. This may be expressed by defining an enhancement parameter

$$\eta = R_M/(R_M)_{\text{Korr}} \simeq \tau_e/\hbar N(E_F) , \tag{24}$$

which is a measure of the tendency for the electrons to localize on a particular site. Since $(R_M)_{\text{Korr}}$ may be computed easily from measured values of $\mathcal{K}$ by means of Eq. (18), η may be determined from measurements of R_M. Furthermore, if $N(E_F)$ can be estimated from the Knight shift value, the residence time τ_e may be obtained from Eq. (23) or (24).

The sensitivity of R_M to the microscopic dynamics of the conduction electrons exhibited by Eq. (23) represents a major virtue of NMR experiments on liquid semiconductors. As compared to the macroscopic transport properties (σ, R_H, α, etc.), the parameters η and τ_e provide a relatively direct measure of localization of the conduction electrons from the point of view of the time during which they reside on a nuclear site.

b. Quadrupolar relaxation. In any liquid diffusional and vibrational thermal motions of atoms or ions produce fluctuating electric field gradients at the nucleus. In addition, rotational modes also modulate the local field gradients in liquids composed of molecules or other relatively stable atomic associations. These time-dependent electric field gradients can provide an important source of spin-lattice relaxation for nuclei possessing electric quadrupole moments.[41]

Calculation of the appropriate correlation functions [Eq. (11)] for quadrupolar interactions in liquids is very difficult owing to the current incomplete state of knowledge of the complex microscopic dynamics of the liquid state. For the purposes of this paper it is sufficient to employ the approximate form given by Eq. (14) which becomes[34]

$$R_Q = \tfrac{3}{40} f(I)(eQ/\hbar)^2\{\delta V_{zz}^2\}\tau_i , \tag{25}$$

where δV_{zz} is the instantaneous fluctuation of the electric field gradient and τ_i is a correlation time for the appropriate ionic motion. Since all other parameters are known, τ_i could be obtained from measurements of R_Q if an independent determination of $\{\delta V_{zz}^2\}$ is available, for example, from static quadrupolar effects in the solid state of the system of interest or in a closely related solid.

A common characteristic of liquid semiconductors appears to be preservation of a marked degree of local atomic order above T_m.[42] This implies the existence of molecular associations which are long lived in comparison with those in pure liquid metals or liquid alloys. The quadrupolar correlation time τ_i thus acquires particular importance in liquid semiconductors since it corresponds to the lifetime of a particular local arrangement of ions.

III. EXPERIMENTAL METHODS

The samples used in these experiments were commercially prepared[43] from 99.999% pure elemental materials. In order to ensure adequate penetration of the radio-frequency field into the samples, powdered sample material was mixed in roughly equal proportions with powdered quartz. This procedure was sufficient to maintain separation between the sample particles in the liquid state. The mixtures were sealed under vacuum in quartz vials for the experimental runs.

High temperatures were obtained in a cylindrical furnace employing a platinum heating element wound noninductively on an alumina ceramic form. The single platinum rf coil was embedded in the inner wall of a cast alumina cylinder which fitted closely around the sample vial. Sample temperatures were measured with Pt vs Pt–10% Rh thermocouples and the accuracy, including the thermal gradient over the sample volume, was at least ±4 K over the temperature range covered. The temperature was stabilized with a simple regulation system employing a thermocouple as sensor. The stability during application of rf pulses (5-μsec pulse width at 200 pulse repetitions per sec) was better than ±0.1 K.

Nuclear resonance signals were observed at frequencies of 9.0, 10.2, and 16.0 MHz using coherent pulsed NMR techniques. The amplitude of the rf magnetic field was normally 40–60 G. Knight shifts were measured relative to the resonance position of appropriate ions in reference solutions. These were (i) aqueous solution of $In_2(SO_4)_3$ for In^{115}, (ii) aqueous solution of $GaCl_3$ for Ga^{69} and Ga^{71}, (iii) $HSbF_6$ for Sb^{121} and Sb^{123}, and (iv) a solution of TeO_2 in HCl for Te^{125}. In each case the reference solution was made sufficiently dilute that the resonance position became independent of concentration.

Measurement of spin-lattice relaxation time T_1 was difficult for the liquids studied owing to the unusually rapid relaxation rates encountered ($1/T_1 \gtrsim 10^5$ sec). Under these conditions we found that the spin-spin relaxation time T_2 could be measured from the free-induction decay with greater precision than was obtainable from standard two-pulse T_1 measurements. Under the conditions of extreme narrowing ($\omega_0\tau \ll 1$) applicable to these liquids, we are justified in taking[44]

$$R = 1/T_1 = 1/T_2 \,. \tag{26}$$

The equality of T_1 and T_2 was checked in a few cases and found to hold to within the ±25% accuracy of the T_1 measurements. The magnetic and quadrupolar rates R_M and R_Q for the Ga and Sb isotopes were obtained from measured values of R by means of Eqs. (15a)–(15d).

IV. EXPERIMENTAL RESULTS

NMR signals were observed for In^{115}, $Ga^{69,71}$, and $Sb^{121,123}$ in In_2Te_3, Ga_2Te_3, and Sb_2Te_3 at temperatures ranging from roughly 150 K below the respective melting points to 1500 K (1400 K for Sb_2Te_3). The lower limits of these ranges were imposed by vanishing signal amplitudes probably caused by the onset of quadrupolar broadening in the solids at low temperatures. The high-temperature limit was determined by onset of chemical reactions between the sample materials and the supporting quartz powders. Because of poor signal-to-noise ratios and the general invalidity of Eq. (26) in solids, meaningful relaxation-rate measurements were not obtained below T_m for these nuclei.

The Te^{125} resonance signals were very weak due to the low abundance (7.03%) and low spin ($I = \frac{1}{2}$) of this isotope. Although Te^{125} has no quadrupole moment, measurements on this isotope in the solids were also limited to temperatures near T_m. At lower temperatures long spin-lattice relaxation time made observation of the Te^{125} resonance increasingly difficult. Because of the over-all low quality of the Te^{125} signals, measurements on this resonance were limited to Knight shifts.

For each sample the melting transition was marked by discontinuites in the Knight shifts and linewidths. The temperatures at which these transitions occurred lie within 5 K of values of the melting points given in the literature[45] for the stoichiometric compounds.

A. In_2Te_3

Knight shift data for In^{115} ($\mathcal{K}^{115}$) and Te^{125} ($\mathcal{K}^{125}$) in solid and liquid In_2Te_3 are shown in Fig. 2. We call particular attention to the following features of the data. The small temperature-independent

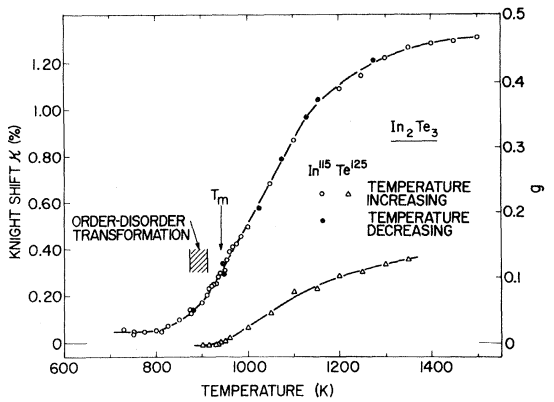

FIG. 2. Knight shifts $\mathcal{K}^{115}$ and $\mathcal{K}^{125}$ for In^{115} and Te^{125} on In_2Te_3 as functions of temperature. Right-hand ordinate shows density-of-states reduction factor g.

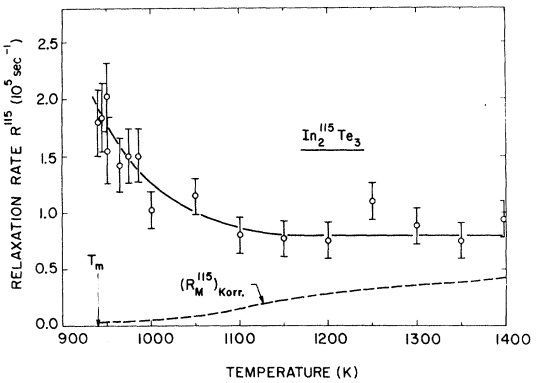

FIG. 3. Nuclear relaxation rate R^{115} for In^{115} in In_2Te_3 as a function of temperature. Dashed line represents Korringa relaxation rate $(R_M^{115})_{Korr}$ calculated from experimental Knight shifts and Eq. (18).

values of $\mathcal{K}$ at the lowest temperatures correspond to expectations for an intrinsic semiconductor at low temperatures. For Te^{125} the small value of $\mathcal{K}^{125}$ persists up to T_m (940 K) whereas $\mathcal{K}^{115}$ shows a marked increase over a 150-K interval below T_m. The changes in $\mathcal{K}^{115}$ and $\mathcal{K}^{125}$ at T_m are very small (e.g., $\Delta\mathcal{K}^{115} < 0.05\%$). Above T_m both $\mathcal{K}^{115}$ and $\mathcal{K}^{125}$ rise rapidly with temperature and $\mathcal{K}^{115}$ appears to reach a constant value at the highest temperatures obtained. The value of $\mathcal{K}^{125}$ remains much smaller than $\mathcal{K}^{115}$ over the entire temperature range covered. The temperature dependence of $\mathcal{K}^{115}$ was reversible with respect to heating and cooling in both solid and liquid states.

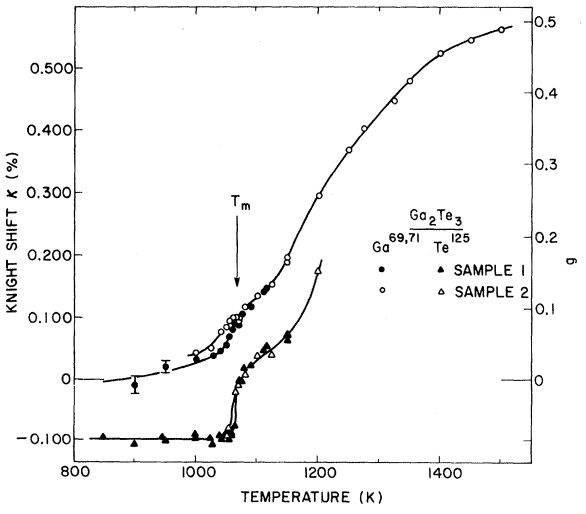

FIG. 4. Knight shifts $\mathcal{K}^{69,71}$ and $\mathcal{K}^{125}$ for Ga^{69}, Ga^{71}, and Te^{125} in Ga_2Te_3 as functions of temperature. Data were taken for sample No. 1 during initial heating of the sample; sample No. 2 was cycled repeatedly through T_m before data were taken below T_m. Right-hand ordinate shows density-of-states reduction factor g.

The total relaxation rate R^{115} for In^{115} in In_2Te_3 is plotted in Fig. 3. Near T_m the observed relaxation rate is very high and, for example, exceeds by more than an order of magnitude the value of R^{115} in liquid InSb.[35] In this temperature range R^{115} exceeds the calculated Korringa rate $(R_M^{115})_{Korr}$ by about two orders of magnitude while at higher temperatures R^{115} decreases and begins to approach $(R_M^{115})_{Korr}$.

B. Ga_2Te_3

Knight shift data for $Ga^{69,71}$ and Te^{125} in solid and liquid Ga_2Te_3 are shown in Fig. 4. Within experimental error the observed shifts were the same for the two Ga isotopes and the plotted values $\mathcal{K}^{69,71}$ represent the average of the measured shifts $\mathcal{K}^{69}$ and $\mathcal{K}^{71}$ at each temperature. The range of the data for $\mathcal{K}^{125}$ was limited by deteriorating signal-to-noise ratios for Te^{125} above 1200 K in this material. The temperature dependence of the data is strikingly similar to that of In_2Te_3. The magnitude of $\mathcal{K}^{69,71}$ is understandably smaller than $\mathcal{K}^{115}$ since the hyperfine coupling strength increases with increasing atomic number.[30] The principal difference between the data for the two systems is the larger negative value of $\mathcal{K}^{125}$ in solid Ga_2Te_3, and its rather sharp increase at T_m (1065 K). Above T_m the magnitudes and temperature dependences of $\mathcal{K}^{125}$ are closely similar in In_2Te_3 and Ga_2Te_3.

Effects related to the thermal history of the sample were investigated by measuring $\mathcal{K}^{69,71}$ both for a sample (No. 2) which had been cycled many times through T_m and a sample (No. 1) for which data were taken as the material was heated for the first time. As shown in Fig. 4 the effect of repeated melting was a systematic increase in $\mathcal{K}^{69,71}$ just below T_m, whereas no appreciable dependence on sample history was observed above T_m.

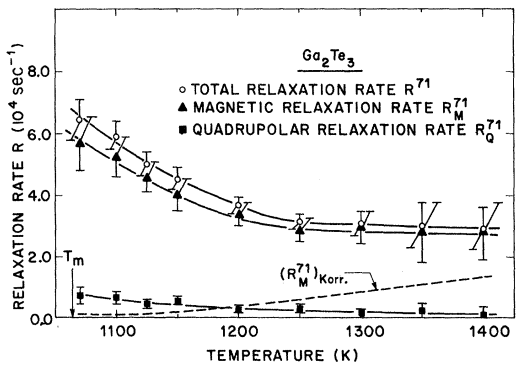

FIG. 5. Total nuclear relaxation rate R^{71}, magnetic rate R_M^{71}, and quadrupolar rate R_Q^{71} for Ga^{71} in Ga_2Te_3 as functions of temperature. Dashed line represents Korringa relaxation rate $(R_M^{71})_{Korr}$ calculated from experimental Knight shifts and Eq. (18).

Relaxation rates for Ga^{71} in liquid Ga_2Te_3 (R^{71}) are shown in Fig. 5. Also shown are the magnetic and quadrupolar rates (R_M^{71} and R_Q^{71}, respectively) computed from measured values at R^{69} and R^{71} and the Korringa rate $(R_M^{71})_{Korr}$ computed from Eq. (18). The decomposition shows that the Ga^{71} relaxation rate is mainly due to magnetic processes whose strength exceeds the Korringa rate by more than two orders of magnitude near T_m. The value of R_M^{71} approaches the Korringa rate at the highest temperatures as was also observed for the total rate R^{115} in In_2Te_3. The quadrupolar rate decreases somewhat more rapidly with increasing temperature and could barely be resolved at 1400 K.

C. Sb_2Te_3

Knight shifts for $Sb^{121,123}$ and Te^{125} in solid and liquid Sb_2Te_3 are shown in Fig. 6. These data contrast with those for In_2Te_3 and Ga_2Te_3 in several respects. A surprisingly large value of $\mathcal{K}^{121,123}$ was observed below T_m (889 K) and this value was nearly independent of temperature. There is a small drop in $\mathcal{K}^{121,123}$ just below T_m followed by a small but sharp increase at the melting transition. As the temperature was raised in the liquid range only a modest increase in $\mathcal{K}^{121,123}$ was observed. The value of $\mathcal{K}^{125}$ below T_m is very close to its value in Ga_2Te_3 but jumps to a much larger value at the melting point.

The behavior of the resonance signals in the vicinity of T_m was quite complex. The transition at T_m was marked by an appreciable narrowing of the Sb^{121} and Sb^{123} resonance lines. However, the linewidth transition was quite sluggish and occurred over a (20–30)-K interval centered on the expected melting point. The small change in $\mathcal{K}^{121,123}$ was much sharper than this and occurred within 10 K. In contrast, the change in $\mathcal{K}^{125}$ began about 50 K below T_m where two Te^{125} resonance lines could be resolved. The "solid" value of $\mathcal{K}^{125}$ tended to increase slightly in this range while the "liquid" value decreased. Above T_m only one Te^{125} line was observed.

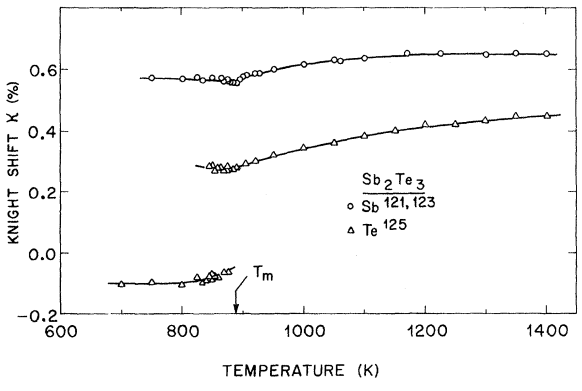

FIG. 6. Knight shifts $\mathcal{K}^{121,123}$ and $\mathcal{K}^{125}$ for Sb^{121}, Sb^{123}, and Te^{125} in Sb_2Te_3 as functions of temperature. Double values of $\mathcal{K}^{125}$ just below T_m apply to two resonance lines observed in this temperature range.

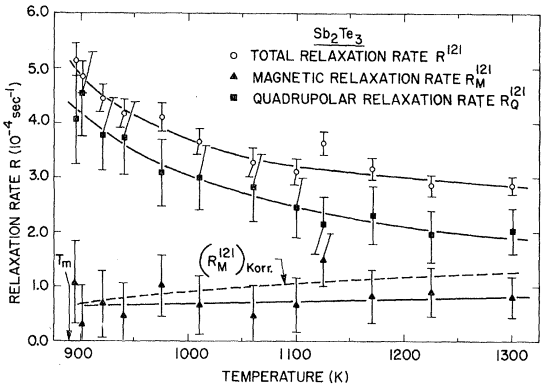

FIG. 7. Total nuclear relaxation rate R^{121}, magnetic rate R_M^{121}, and quadrupolar rate R_Q^{121} for Sb^{121} in Sb_2Te_3 as functions of temperature. Dashed line represents Korringa relaxation rate $(R_M^{121})_{Korr}$ calculated from experimental Knight shifts and Eq. (18).

The total relaxation rate R^{121} and the magnetic and quadrupolar rates R_M^{121} and R_Q^{121} for Sb^{121} are shown in Fig. 7. Here, in contrast with Ga_2Te_3, the majority of the observed relaxation is quadrupolar although the temperature dependence of R_Q^{121} is similar to that of R_Q^{71} in Ga_2Te_3. The small magnetic component R_M^{121} is close to the calculated Korringa value over the whole range of temperatures.

V. DISCUSSION

A. Solid and Liquid Structure: Melting-Point Changes and Quadrupole Relaxation

Knowledge of the atomic arrangement is an important prerequisite to understanding the electronic structure of a metal or semiconductor. We therefore begin our discussion of the experimental results by summarizing the available structural data and relating this to new information obtained from changes in the NMR parameters at T_m and from quadrupolar relaxation above T_m in In_2Te_3, Ga_2Te_3, and Sb_2Te_3.

In_2Te_3 and Ga_2Te_3 crystallize in a defect zinc-blende structure[45] in which $\frac{1}{3}$ of the In (Ga) sites are vacant. X-ray and infrared transmission studies[46–48] of both materials have shown that the vacancies exhibit long-range order at 300 K in suitably prepared samples. Investigation of the relation of ordering in In_2Te_3 at 300 K to the thermal history of the material[47] has shown that a transformation to a high-temperature disordered phase occurs roughly 50 K below T_m. Both compounds are semiconductors with electrical gaps[49] of 1.12 eV (In_2Te_3) and 1.7 eV (Ga_2Te_3) below T_m.

Sb_2Te_3 crystallizes in the layer-type Bi_2Te_3 or

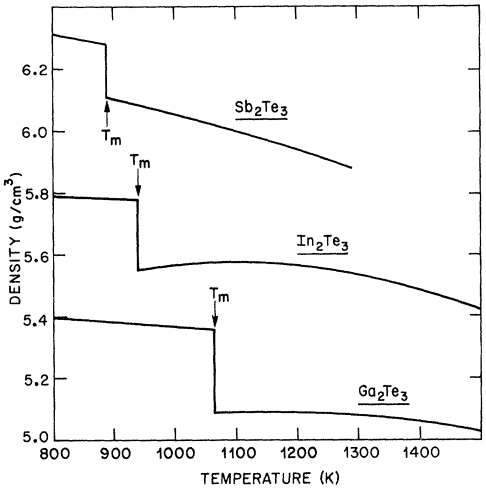

FIG. 8. Density ρ as a function of temperature for Sb_2Te_3, In_2Te_3, and Ga_2Te_3 (Ref. 42).

"tetradymite" structure[42,45] consisting of five-layer packets (Te-Sb-Te-Sb-Te) joined by relatively weak Te-Te bonds.[50] The bonding between packets is believed to be similar to the bonding between chains of Te atoms in crystalline Te.[42] The energy gap (optical) at 300 K is 0.3 eV.[51]

The densities[42] ρ of In_2Te_3, Ga_2Te_3, and Sb_2Te_3 at high temperatures are shown in Fig. 8. All three compounds undergo a decrease in ρ upon melting. Above T_m the densities of In_2Te_3 and Ga_2Te_3 increase slightly with increasing T over an interval of about 150 K before onset of the more normal decrease due to thermal expansion. The behavior of Sb_2Te_3 is more conventional and ρ decreases monotonically with increasing temperature in the liquid.

The electrical conductivities (Fig. 9) of In_2Te_3 and Ga_2Te_3 are 14 and 30 $(\Omega\,\mathrm{cm})^{-1}$, respectively, just above T_m, but rise rapidly in the temperature range in which the density increases. The temperature dependence of σ becomes weaker at temperatures well above T_m. The value of σ for Sb_2Te_3 is relatively high just above T_m and only a modest increase in σ occurs upon heating to higher temperatures.

The melting behavior of In_2Te_3 and Ga_2Te_3 contrasts with that of such semiconductors as Si, Ge, and InSb. The latter materials contract upon melting, increasing the atomic coordination number, and they exhibit metallic conductivity $[\sigma > 10^4(\Omega\,\mathrm{cm})^{-1}]$ immediately above T_m.[42] The expansion of In_2Te_3, Ga_2Te_3, and Sb_2Te_3 on melting suggests that the local atomic arrangement or "short-range order" of these materials tends to be preserved through melting. This idea is supported by the small size of the observed changes in Knight shifts and transport properties. The density maxima exhibited by In_2Te_3 and Ga_2Te_3 imply, however, that an increase in local coordination does occur in these liquids at higher temperatures while there is little indication of further structural modification in Sb_2Te_3.

The quadrupolar relaxation rates provide additional evidence for solidlike short-range order or molecular association in Ga_2Te_3 and Sb_2Te_3. In Table I we compare values of R_Q^{71} and R_Q^{121} just above T_m in Ga_2Te_3 and Sb_2Te_3 with values obtained for the same nuclei in the pure metals and some metallic liquid compounds at comparable temperatures. The quadrupolar rates may be seen to be appreciably higher in the tellurides than in the other systems and, furthermore, this difference is much greater for Ga_2Te_3 than for Sb_2Te_3.

In principle the rapid quadrupolar relaxation of the tellurides could be explained by large values of either $\{\delta V_{zz}^2\}$ or τ_i. However, two factors argue strongly that the latter is the dominant effect. The first is that unusually large values of $\{\delta V_{zz}^2\}$ are required to explain the observed rates if we assume τ_i to be the same as the pure metal. For example, the *static* value of V_{zz} increases by only about $2\frac{1}{2}$ times as one goes from pure solid Ga to the highly ionic insulator $GaCl_3$.[52,53] On the other hand, the observed value of R_Q^{69} in the nearly metallic liquid Ga_2Te_3 requires that the value of δV_{zz} produced by a typical noncubic arrangement of ions in the liquid exceed the static V_{zz} in solid Ga by more than a factor of 8.

The second point is that at very high temperatures R_Q in the tellurides begins to approach the

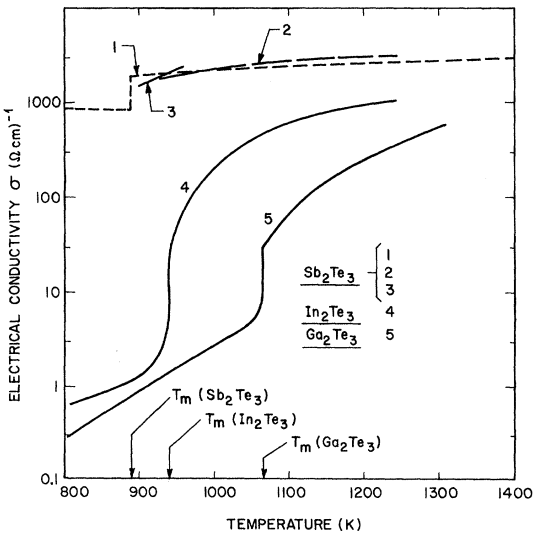

FIG. 9. Electrical conductivity as a function of temperature: Sb_2Te_3 [curve 1, Ref. 42; curve 2, Ref. 54; curve 3, J. E. Enderby and L. Walsh, Phil. Mag. 14, 991 (1966)]; In_2Te_3 (curve 4, Ref. 49); Ga_2Te_3 (curve 5, Ref. 49).

TABLE I. Comparison of quadrupolar relaxation rates and correlation times of Ga^{71} and Sb^{121} in pure liquid metals and some intermetallic compounds.

Isotope	Liquid	T (K)	R_Q (10^3 sec^{-1})	eQV_{zz} (MHz)	τ_i (10^{-12} sec)
Ga^{71}	Ga	1050	0.10[a]	13.73[b]	0.14[c]
	GaSb	1050	$\leq$0.46[a]	13.73	$\leq$0.62[c]
	$AuGa_2$	1050	0.47[d]	13.73	0.63[c]
	Ga_2Te_3	1070	7.0[e]	13.73	9.4[c]
Sb^{121}	Sb	905	3.6[f]	76.9[g]	0.65[c]
	GaSb	940	9.5[a]	76.9	1.7[c]
	InSb	900	13.5[f]	76.9	2.5[c]
	Sb_2Te_3	900	42[e]	76.9	7.7[c]

[a]A. L. Kerlin and W. G. Clark (unpublished).
[b]Reference 52.
[c]Equation (25).
[d]W. W. Warren, Jr. and J. H. Wernick (unpublished).
[e]This research.
[f]Reference 35.
[g]R. R. Hewitt and B. V. Williams, Phys. Rev. 129, 1188 (1963).

values observed in more conventional metallic liquids. This implies that in this temperature range $\{\delta V_{zz}^2\}$ and τ_i are rather weakly dependent on composition. It is easy to understand why τ_i should increase at lower temperatures as a result of slower rotations and diffusion and the formation of larger aggregates of atoms. It is far less clear why $\{\delta V_{zz}^2\}$ should increase dramatically as the temperature is lowered. In summary, while it is difficult (and probably incorrect) to exclude entirely variations in $\{\delta V_{zz}^2\}$ among the various liquids, it is most plausible that the rapid quadrupolar relaxation rates in the liquid tellurides result from rather long values of the ionic correlation time τ_i.

In order to obtain rough numerical estimates of τ_i in the various liquids we have made the simple assumption that the rms field gradient fluctuations in the liquid compounds, $\{\delta V_{zz}^2\}^{1/2}$ are the *same* as the static field gradients V_{zz} in the appropriate pure solid metals. The resulting values of τ_i calculated from Eq. (25) are given in the final column of Table I. The principle feature we wish to emphasize is the systematic lengthening of τ_i as one proceeds from the most metallic liquids (Ga and Sb) to the most "semiconducting" (Ga_2Te_3). This qualitative behavior gives additional support to the notion that low electrical conductivity in the liquid state is associated with the presence of relatively long-lived molecules or other associations of atoms.

B. Knight Shifts and Magnetic Relaxation Rates

The strongly temperature-dependent Knight shifts in In_2Te_3 and Ga_2Te_3 might result from either a temperature-dependent density of states or an increase in the amount of conduction electron s character at higher temperatures. We believe the former effect to be dominant for the following reasons. First, the magnetic susceptibility[42] becomes more paramagnetic while remaining roughly proportional to $\mathcal{K}$ as T increases. This suggests an increase in the density of states since the electron spin susceptibility should not be highly sensitive to the relative s or p character of the wave functions. Similarly, the transport properties σ and α indicate an increase in the number of charge carriers at higher temperatures.[42,49,54] Finally, the relative magnitudes of $\mathcal{K}^{115}$ and $\mathcal{K}^{69,71}$ with respect to $\mathcal{K}^{125}$ are good evidence that the wave functions at the In (Ga) sites are, at T_m, already very much more s-like than those at the Te site. The similarity of the temperature dependences of $\mathcal{K}^{115}$ ($\mathcal{K}^{69,71}$) and $\mathcal{K}^{125}$ indicates that this situation does not change dramatically at higher temperatures. For purposes of estimating the density of states and the parameter g [defined by Eq. (1)] we will assume that the states at the Fermi level have predominantly s character at the In or Ga site at all temperatures in the liquid.

We estimate g for In_2Te_3 by comparing $\mathcal{K}^{115}$ in In_2Te_3 to the value of $\mathcal{K}^{115}$ in the metallic solid InTe II as described in Sec. IIB. The pressure-stabilized metallic phase InTe II is a good metal [$\sigma \simeq 10^4$ $(\Omega\,\mathrm{cm})^{-1}$ at 300 K[55]] and has a large In^{115} Knight shift: $\mathcal{K}^{115}$(InTe II) = 2.79 ± 0.04% at 300 K.[56] Thus according to Eq. (10) we take

$$g \simeq \mathcal{K}^{115}(In_2Te_3)/\mathcal{K}^{115}(\mathrm{InTe\ II}). \tag{27}$$

The resulting values are displayed by scaling the data for $\mathcal{K}^{115}$ in In_2Te_3 on the right-hand ordinate of Fig. 2 and characteristic values are given in Table II.

Unfortunately no data on an appropriate metal are available for comparison with the Ga_2Te_3 Knight shifts. Therefore we used an optical hyperfine value[30] $|\psi_A(0)|^2 = 6\times10^{25}$ cm^{-1} to obtain the density of states and calculated $N(E_F)_{fe}$ from free-electron theory assuming one s electron per Ga ion.[57] The

values of g obtained in this way are shown in Fig. 4 and Table II.

It is interesting and reassuring that the absolute values of g estimated for In_2Te_3 and Ga_2Te_3 are similar in spite of the quite different means employed in obtaining $\langle|\psi(0)|^2\rangle_F$. In both systems g varies smoothly from $g \simeq 0$ in the crystalline semiconductors to $g \simeq 0.5$ far above T_m. Although most of the increase in g occurs in the liquid range, the rise just *below* T_m is particularly interesting. The observed values of $\mathcal{K}^{115}$ and $\mathcal{K}^{69,71}$ in this range are at least an order of magnitude larger than might be expected from thermally excited carriers with a 1-eV gap. The fact that the signals are quite weak in this temperature range suggests that the resonances observed might be due to small amounts of Te-rich material in the sample mixture. An alternative explanation is that an appreciable number of states is introduced into the energy gap above the order-disorder transformation. The widths of these rises in $\mathcal{K}^{115}$ and $\mathcal{K}^{69,71}$ might then reflect the high sensitivity of the ordering temperature reported[58] for very small departures from stoichiometry.

The negative temperature-independent value of $\mathcal{K}^{125}$ in solid Ga_2Te_3 appears to be a chemical shift with respect to the reference compound (TeO_2 in HCl solution). It is interesting that there is no increase in $\mathcal{K}^{125}$ coincident with the rises in $\mathcal{K}^{115}$ and $\mathcal{K}^{69,71}$ just below T_m in In_2Te_3 and Ga_2Te_3. This means that those states responsible for the observed values of $\mathcal{K}^{115}$ and $\mathcal{K}^{69,71}$ in this range have appreciable s-wave character only at the In (Ga) sites.

In the case of Sb_2Te_3 a slightly different situation occurs. Here $\mathcal{K}^{121,123}$ is nearly constant at a metallic value over the solid range covered while $\mathcal{K}^{125}$ is small and negative, as in Ga_2Te_3. The large value of $\mathcal{K}^{121,123}$ may be a result of departure from stoichiometry which is known to markedly increase the conductivity of Sb_2Te_3.[42] Whatever their origin, the states responsible for the $Sb^{121,123}$ shifts in solid Sb_2Te_3 also have s character only at Sb positions.

For liquid Sb_2Te_3 there is no evidence of a strongly temperature-dependent density of states. Since there is good reason to expect p-electron effects to be more important for pentavalent Sb than for trivalent In and Ga, we have not attempted to obtain a numerical value for $N(E_F)$ from $\mathcal{K}^{121,123}$ in Sb_2Te_3. (The relatively large role of p-electron effects in Sb_2Te_3 can be seen from the much larger ratio $\mathcal{K}^{125}/\mathcal{K}^{121,123}$ in Sb_2Te_3 compared to, say, $\mathcal{K}^{125}/\mathcal{K}^{115}$ in In_2Te_3.) We point out, however, that $\mathcal{K}^{121,123}$ in Sb_2Te_3 is within 20% of its values in liquid Sb and InSb.[35] Both of the latter liquids are good metals and may be assumed to have values of $N(E_F)$ close to the free-electron value.

The behavior of the nuclear relaxation rates serves to further distinguish In_2Te_3 and Ga_2Te_3 from Sb_2Te_3. The very large enhancement of R_M relative to $(R_M)_{Korr}$ near T_m in In_2Te_3 and Ga_3Te_3 means that the conduction electrons in these liquids are strongly disposed to remain near a particular nuclear position. The magnitudes of the enhancement factors η and correlation times τ_e calculated from Eq. (24) (Table II) show, in fact, that the electrons are localized for "residence times" more than two orders of magnitude longer than appropriate for NFE with the same density of states. In contrast, R_M^{121} in Sb_2Te_3 agrees with the Korringa predictions (i.e., $\eta \simeq 1$) at all temperatures and there is no evidence of a large departure from NFE dynamics.

TABLE II. Characteristic values of the density-of-states reduction factor g, the magnetic relaxation-rate enhancement factor η, and the electronic correlation time τ_e for liquid In_2Te_3 and Ga_2Te_3.

T (K)	g	η	$\tau_e(10^{-15}$ sec)
		In_2Te_3	
950	0.12	100[a]	1.81[a]
1025	0.21	17[a]	0.54[a]
1100	0.31	6.0[a]	0.28[a]
1250	0.41	2.9[a]	0.18[a]
1400	0.46	2.0[a]	0.14[a]
		Ga_2Te_3	
1070	0.086	151	1.87
1125	0.13	49	0.93
1200	0.25	9.3	0.34
1300	0.37	3.5	0.19
1400	0.45	2.1	0.14

[a]Not corrected for quadrupolar relaxation.

C. Comparison of Experiment and Theoretical Models

The two most relevent NMR parameters for testing the validity of the theoretical models are (i) the magnitude of the In (Ga, Sb) Knight shift or equivalently, g, and (ii) the magnetic relaxation enhancement η. In this subsection we describe what we believe to be the state of consistency between these parameters measured for In_2Te_3, Ga_2Te_3, and Sb_2Te_3 and the theoretical models described in Sec. II. The results of these comparisons are summarized in Table III.

It is quite clear that conventional semiconductor theory is inappropriate for the liquids we have considered. The magnitudes of the Knight shifts are much too large to be explained by intrinsic concentrations of thermally excited carriers for values of the energy gap which are comparable to those of the crystalline solids. Moreover, even if the carrier concentrations were very high owing to high concentrations of donors or acceptors, the holes

TABLE III. Agreement of the observed magnitudes of Knight shift $\mathcal{K}$ and relaxation enhancement η with three models: conventional semiconductor theory (CST), pseudogap model (PG), and pseudobinary alloy (PBA).

	In_2Te_3		Ga_2Te_3		Sb_2Te_3	
MODEL	$\mathcal{K}$	η[a]	$\mathcal{K}$	η	$\mathcal{K}$	η
CST	No	No ?	No	No	No	Yes
PG	Yes	Yes ?	Yes	Yes	Yes	Yes
PBA	Yes	No ?	Yes	No	Yes	Yes

[a]Interpretation of η for In_2Te_3 is ambiguous because of possible uncorrected quadrupolar contributions.

and electrons would behave as free carriers and no enhancement of the relaxation rate would be expected. This result is in accord with Allgaier's conclusion[1] that the Hall and Seebeck coefficients of many liquid semiconductors are inexplicable within the framework of standard semiconductor concepts as conventionally applied to crystalline materials.

The pseudobinary alloy model is in general agreement with the Knight shift data since a minimum in the density of states of the "free" band permits values of $N(E_F)$ with any magnitude less than or on the order of $N(E_F)_{fe}$. However, the enhanced relaxation rates present a serious problem for this model. As we have discussed, electron dynamics are described for the pseudobinary alloy in terms of scattering of NFE with an energy-dependent mean free path Λ. Now Λ must be presumed (as in Ref. 22) to be at least as large as one interatomic spacing since the concept of a mean free path (as it is normally employed in scattering theory) loses meaning when the mean free path becomes less than the distance between scattering centers. But according to the arguments presented in Sec. IIB, one would not expect to see large enhancements of the relaxation rates in In_2Te_3 and Ga_2Te_3 if such a NFE model represented an appropriate description of the electron dynamics. We conclude, therefore, that the pseudobinary alloy model in its present form does not provide an adequate picture of the electron dynamics in liquid In_2Te_3 and Ga_2Te_3. On the other hand, no relaxation enhancement was observed for Sb_2Te_3 and the data appear to be consistent with the model for this liquid.

Of the three models we have considered, the pseudogap model is most capable of explaining the essential features of our experimental results. Estimates of g from the observed Knight shifts indicate a relatively deep pseudogap ($g \simeq 0.1$) just above T_m in In_2Te_3 and Ga_2Te_3 while g is probably at least 0.5 at T_m in Sb_2Te_3. According to this interpretation, the temperature dependence of $\mathcal{K}^{115}$ and $\mathcal{K}^{69,71}$ in In_2Te_3 and Ga_2Te_3 indicates that the pseudogap "fills in" at higher temperatures as a result of collapse of the local "molecular" arrangement, increase of the coordination number, and mixing of the In (Ga) "sublattices." This notion is supported both by the temperature dependence of the densities and by the behavior of the quadrupolar relaxation rates. For Sb_2Te_3 the pseudogap is much less pronounced at T_m and changes only modestly with temperature.

The observed enhancement of the magnetic relaxation rates in In_2Te_3 and Ga_2Te_3 is in good agreement with what might be expected from the formation of localized states when the pseudogap is deep. The data show that as the density of states decreases, the electrons increasingly tend to remain on a particular nuclear site. In the following sections we extend these qualitative conclusions and make some quantitative comparisons among the observed NMR results, dc conductivity, and predictions made by Mott on the basis of the pseudogap model.

D. Relationship of NMR Results to dc Conductivity

The electrical conductivity[49] and magnetic relaxation-rate enhancements for In_2Te_3 and Ga_2Te_3 are shown in Fig. 10 plotted vs g with temperature as an intrinsic parameter. When plotted in this manner the data for the two liquids are strikingly similar in spite of possible quadrupolar contributions to σ for In_2Te_3. A rather abrupt change in the slopes of these curves occurs at a value g_c, where

$$g_c = 0.18 \pm 0.03 \ .$$

As g decreases below g_c, sharply rising values of

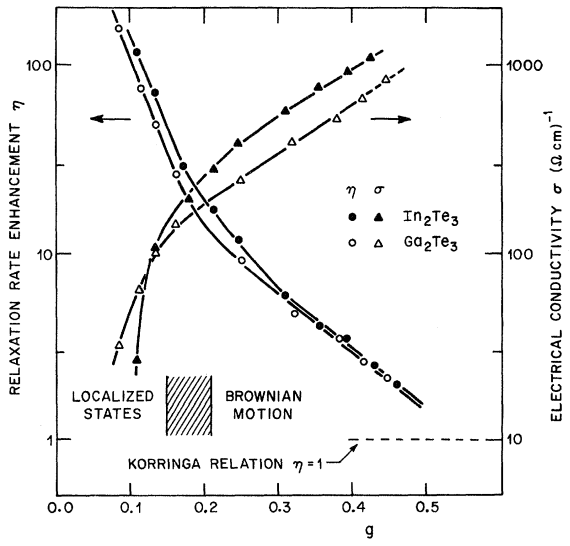

FIG. 10. Magnetic relaxation enhancement η and electrical conductivity σ versus density-of-states reduction factor g for In_2Te_3 and Ga_2Te_3. Temperature is the implicit parameter.

η indicate that the electrons rapidly become more localized while, in the same range, the conductivity drops sharply. Above g_c, on the other hand, σ increases with g much more slowly and η approaches the NFE value ($\eta = 1$).

We caution that the present experiments do not demonstrate that the electronic states below g_c are localized in the rigorous sense. That is, we have not shown that the wave functions of these states are damped exponentially at distances far from a particular site or that the dc conductivity vanishes at 0 K. On the other hand, we have established that just above T_m the mobility of an electron with respect to a given nucleus has dropped by more than two orders of magnitude below the expectation for NFE. Furthermore, this effect is clearly reflected in the macroscopic transport by the drop in σ below g_c. Such behavior is exactly what one might expect for a transition from extended states to weakly localized states at finite temperatures. There is no hint in the data that the trend towards increasingly strong localization does not continue to values of g smaller than the minimum values obtainable in these liquids. From the operational point of view of describing electronic transport at finite temperatures, therefore, the states in the pseudogap can be identified by their "residence times" as effectively localized when $g < g_c$, regardless of the exact quantum-mechanical nature of the eigenstates.

Theoretical estimates made by Mott for the onset of localization in the pseudogap are in quite good agreement with the transition we observe at g_c. His predicted value of $g_c \simeq 0.285$ is approximately 50% higher than our observed value. This cannot be regarded as a serious discrepancy given both the uncertainty in the absolute value of the measured g and the approximate nature of the arguments invoked in Mott's estimate of g_c. As a second point of contact between theory and experiment we note that the value of σ at the localization onset

$$\sigma_c = 200 \pm 70\ (\Omega\,\mathrm{cm})^{-1}$$

compares favorably with various values in the range 100–300 $(\Omega\,\mathrm{cm})^{-1}$ given by Mott[9,12,16] as the minimum possible value for conductivity by extended states.

The high-temperature region of our experiments corresponding to values of g for In_2Te_3 and Ga_2Te_3 in the range $g_c \lesssim g \lesssim 0.5$ represents a transitional regime linking the localized state regime with the metallic regime in which the Korringa relation should be valid. In terms of the relaxation enhancement observed for In_2Te_3 and Ga_2Te_3, the transitional range corresponds to values of η between 1 and 20. Cohen[59] has suggested the existence of such a transitional region in which electron transport proceeds by a kind of diffusion or "Brownian motion" involving very rapid jumps between neighboring lattice sites. As compared with the localized regime the electron states in the Brownian motion regime are extended and electronic transport does not rely on phonon assistance.

On the basis of these considerations we can identify three distinct ranges of electrical conductivity for liquid semiconductors. The first is the regime of metallic conduction in which the conductivity may be characterized by a mean free path and calculated according to scattering theory as in the Faber-Ziman theory[60] for liquid alloys. In this range the nuclear relaxation rate should be independent of the conductivity and the Korringa relation should be obeyed to the extent typical of pure liquid metals (i.e., within about a factor of 2).

The second and third ranges are the Brownian motion and localized state regimes. Here the conductivity may not be described in terms of a mean free path but rather by an equation of the form[12,14,59]

$$\sigma = 2N(E_F)\Omega^{-1}kTe\mu\ , \tag{28}$$

where Ω is the atomic volume and the mobility μ is related to a jump time τ by an Einstein relation

$$\mu = \frac{1}{6}\frac{ed^2}{kT}\frac{1}{\tau}\ . \tag{29}$$

In the Brownian motion regime the jump distance d should be the same as the interatomic spacing a whereas, in the localized regime, d may be greater than a. This increase in d is, of course, offset by longer values of τ leading to reduced mobilities in the localized regime. Now, according to the arguments developed in Sec. II B, the jump time is given by the NMR correlation time τ_e for Brownian motion or for weakly localized states. This correspondence then leads to a simple relation connecting σ and the relaxation enhancement η in these two regimes. Thus, combining Eqs. (28) and (29), we obtain

$$\sigma = \frac{1}{3}\left(\frac{e^2d^2}{\Omega}\right)\frac{N(E_F)}{\tau_e}\ , \tag{30}$$

which gives on substitution of Eq. (24)

$$\sigma\eta = \sigma_0 = e^2d^2/3\Omega\hbar\ . \tag{31}$$

Since a^2/Ω varies little from liquid to liquid, σ_0 should be a universal constant in the Brownian motion regime, whereas increases in d may lead to larger values of σ_0 for localized states. The value of the conductivity at the transition from NFE (metallic) behavior to Brownian motion should be $\sigma_0 \simeq 1500\ (\Omega\,\mathrm{cm})^{-1}$ for typical values $d = 2.5$ Å and $\Omega = 35$ Å^3.

The foregoing ideas are tested in Fig. 11 where

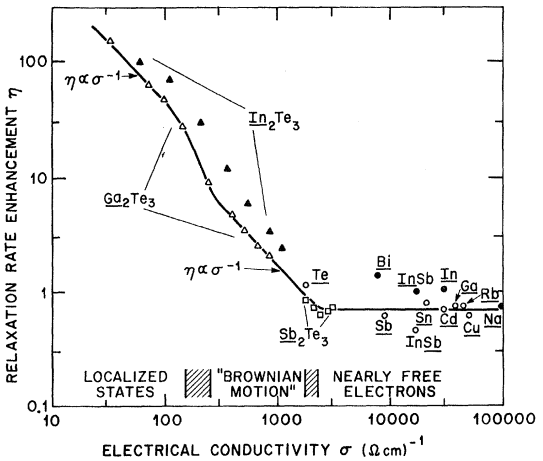

FIG. 11. Magnetic relaxation enhancement η versus electrical conductivity σ for liquid metals and semiconductors. Temperature is the implicit parameter. Relaxation-rate enhancement refers to the underlined atomic species. Open points denote enhancement of magnetic relaxation rate only; closed points apply to systems for which η includes quadrupolar contributions. The solid line is fitted to the nonquadrupolar data with the constraints that η is constant in the NFE regime and $\eta \propto \sigma^{-1}$ in the Brownian motion and localized state regimes.

the relaxation-rate enhancement is plotted versus the conductivity for those liquid metals and semiconductors for which data are available. Considering for the moment only liquids for which η includes no quadrupolar contribution (open points), the three ranges of conductivity are quite evident. For liquids with $\sigma \gtrsim 2000\ (\Omega\text{cm})^{-1}$, η is independent of σ and, for most of the liquids, $\eta \simeq 0.7$. For Ga_2Te_3, on the other hand, η is proportional to σ^{-1} in both the Brownian motion and localized regions. The proportionality constant σ_0 in the Brownian motion regime is $1800 \pm 200\ (\Omega\text{cm})^{-1}$, in good agreement with the value predicted by Eq. (31). In the range of localization σ_0 increases to $4000 \pm 400\ (\Omega\text{cm})^{-1}$. It is interesting to note that according to this scheme Sb_2Te_3 just spans the transition from NFE to Brownian motion transport behavior.

Finally we remark on those cases for which η contains unknown contributions from quadrupolar relaxation (In_2Te_3, InSb, Bi, etc.). The data for these nuclei show the same qualitative behavior as for the "magnetic only" cases except that η is systematically larger. This, of course, is what one expects since quadrupolar relaxation leads to higher values of R relative to $\mathcal{K}$ and, hence, to a larger apparent enhancement factor η.

VI. SUMMARY

Knight shifts and nuclear relaxation rates have been measured for three "liquid semiconductors": In_2Te_3, Ga_2Te_3, and Sb_2Te_3. The strongly temperature-dependent shifts $\mathcal{K}^{115}$ and $\mathcal{K}^{69,71}$ in In_2Te_3 and Ga_2Te_3, respectively, are attributed mainly to a temperature-dependent density of states at the Fermi level. The value of $N(E_F)$ begins to increase below T_m in the vicinity of the order-disorder transformation for In (Ga) vacancies. In the liquids, $N(E_F)$ rises from a value of about $\frac{1}{10}$ of the free-electron density of states near T_m to about $\frac{1}{2}$ the free-electron value at 1400 K. The correlation of this rise in $N(E_F)$ with an increase in density and a decrease in the quadrupolar relaxation rate suggests that a minimum in the density of states (pseudogap) gradually "fills in" as a result of collapse of the local solidlike structure.

Nuclear relaxation rates for In^{115}, Ga^{69}, and Ga^{71} near T_m in liquid In_2Te_3 and Ga_2Te_3 are greatly enhanced with respect to the normal Korringa rates calculated from the Knight shifts. The enhancement exceeds two orders of magnitude just above T_m but drops rapidly with increasing temperature. Decomposition of Ga_2Te_3 total relaxation rates into magnetic and quadrupolar components shows the enhanced relaxation to be magnetic in origin. It was demonstrated from correlation function arguments that such an enhancement may be expected as the conduction electrons become localized on individual nuclear sites.

The data for Sb_2Te_3 contrast sharply with those for In_2Te_3 and Ga_2Te_3. A large $Sb^{121,123}$ shift below T_m is virtually unchanged on melting and only a slight rise in $\mathcal{K}^{121,123}$ occurs as the temperature is raised above T_m. The magnitude of $\mathcal{K}^{121,123}$ indicates that $N(E_F)$ is close to the free-electron value at all temperatures in the liquid. No enhancement of the Sb^{121} magnetic relaxation rates was observed and we conclude from this that there is no significant localization of the conduction electrons in Sb_2Te_3. The Te^{125} shift exhibited a premelting effect and two resonance lines were observed over a 50-K interval below T_m.

The experimental results in In_2Te_3, Ga_2Te_3, and Sb_2Te_3 have been compared with three models for the electronic structure of liquid semiconductors: (a) conventional semiconductor theory, (b) pseudogap model, and (c) pseudobinary alloy model. Of these, only the pseudogap model invokes localization of the electronic states and appears capable of explaining the enhanced relaxation in In_2Te_3 and Ga_2Te_3. The data for Sb_2Te_3 are consistent with either the pseudogap model or the pseudobinary alloy model.

A change in the variation of relaxation enhancement η with changing values of the density-of-states reduction factor g indicates the onset of localization in In_2Te_3 and Ga_2Te_3 occurs when g falls below about 0.2. This onset coincides with sharp drops in the conductivities of both liquids. We must reemphasize, however, the inexact nature of our de-

termination of the absolute value of g since we have utilized rather crude estimates of the hyperfine coupling strength. On the other hand, the transition to localized states is seen mainly from correlation of the values of η and σ with relative changes in g. Thus, the existence of the localization onset is more reliably established than is the precise value of g at which it occurs.

Correlation of the conductivity σ with the magnetic relaxation-rate enhancement η for a number of liquid metals and semiconductors demonstrates the existence of a second transition separating true metallic behavior from a range of conduction by diffusion or "Brownian motion." We suggest therefore that electron conduction in liquids may be classified according to the following three types: (I) metallic conductivity: $\sigma \geq 2000\ (\Omega\,\mathrm{cm})^{-1}$, $\eta \simeq 1$; (II) Brownian motion: $200 \leq \sigma \leq 2000\ (\Omega\,\mathrm{cm})^{-1}$, $1 \leq \eta \leq 20$; (III) localized states: $\sigma \leq 200\ (\Omega\,\mathrm{cm})^{-1}$, $\eta \geq 20$. This classification corresponds quite closely to a scheme proposed by Allgaier on the basis of the magnitudes and temperature dependences of various transport properties. In that case the intermediate region linking metallic and localized behavior (denoted "Class B" in Ref. 1) is slightly wider, encompassing liquids whose conductivities lie in the range $100 \leq \sigma \leq 5000\ (\Omega\,\mathrm{cm})^{-1}$. Enderby and Collings[23] have suggested a somewhat different classification involving two regions defined by conductivities which are either less than or greater than about $1000\ (\Omega\,\mathrm{cm})^{-1}$. Their low-conductivity region (denoted "Type 2") corresponds roughly to our regions II and III.

Of the liquids studied in these experiments, In_2Te_3 and Ga_2Te_3 range from region III to region II as the temperature is raised. The properties of Sb_2Te_3 are only weakly dependent on temperature and this liquid appears to fall right on the transition between regions I and II. Although all three liquids have been called liquid semiconductors in the literature, it would appear that if this appellation is appropriate at all, it should be applied only to In_2Te_3 and Ga_2Te_3 in region III. However, liquids in this range form a unique class and their properties cannot be adequately described with standard semiconductor concepts.

We believe that future NMR studies will prove to be of value in further investigation of microscopic transport in electronically conducting liquids. Such studies would benefit greatly from the availability of a more precise theory of nuclear relaxation for liquids in ranges II and III.

ACKNOWLEDGMENTS

The author expresses his gratitude to N. F. Mott for a stimulating discussion and continuing correspondence during the course of this work. He is indebted to P. W. Anderson and J. Tauc for valuable discussions. R. W. Shaw kindly read the manuscript and provided a number of helpful suggestions. Expert technical assistance by G. F. Brennert is gratefully acknowledged. Finally, he wishes to thank A. L. Kerlin and W. G. Clark for permission to include in Table I their unpublished results for liquid Ga and GaSb.

[1]For an excellent summary of the transport properties of liquid metals and semiconductors see R. S. Allgaier, Phys. Rev. 185, 227 (1969).

[2]Preliminary reports of our work on In_2Te_3 and Ga_2Te_3 have been presented, respectively, in W. W. Warren, Jr., J. Non-Cryst. Solids 4, 168 (1970) and Solid State Commun. 8, 1269 (1970).

[3]A. F. Ioffe and A. R. Regel, Progr. Semicond. 4, 239 (1960).

[4]M. Cutler and C. E. Mallon, J. Appl. Phys. 36, 201 (1965).

[5]M. Cutler and C. F. Mallon, Phys. Rev. 144, 642 (1966).

[6]M. Cutler and M. B. Field, Phys. Rev. 169, 632 (1968).

[7]J. M. Donally and M. Cutler, Phys. Rev. 176, 1003 (1968).

[8]M. Cutler and R. L. Peterson, Phil. Mag. 21, 971 (1970).

[9]N. F. Mott and R. S. Allgaier, Phys. Status Solidi 21, 343 (1967).

[10]N. F. Mott, Phil. Mag. 17, 1259 (1968).

[11]N. F. Mott and E. A. Davis, Phil. Mag. 17, 269 (1968).

[12]N. F. Mott, Phil. Mag. 19, 835 (1969).

[13]N. F. Mott, Contemp. Phys. 10, 125 (1969).

[14]N. F. Mott, Festkoerperprobleme 9, 22 (1969).

[15]N. F. Mott, Phil. Mag. 22, 7 (1970).

[16]N. F. Mott (unpublished).

[17]P. W. Anderson, Phys. Rev. 109, 1492 (1958).

[18]A. I. Gubanov, *Quantum Electron Theory of Amorphous Conductors* (Consultants Bureau, New York, 1965).

[19]L. Banyai, *Physique des Semiconducteurs* (Dunod, Paris, 1964), p. 400.

[20]M. H. Cohen, H. Fritzsche, and S. R. Ovshinsky, Phys. Rev. Letters 22, 1065 (1969).

[21]E. N. Economou, S. Kirkpatrick, M. H. Cohen, and T. P. Eggarter, Phys. Rev. Letters 25, 520 (1970).

[22]J. E. Enderby and C. J. Simmons, Phil. Mag. 20, 125 (1969).

[23]J. E. Enderby and E. W. Collings, J. Non-Cryst. Solids 4, 161 (1970).

[24]J. M. Ziman, *Principles of the Theory of Solids* (Cambridge U. P., London, 1964), p. 202.

[25]Reference 24, pp. 183–185.

[26]C. P. Slichter, *Principles of Magnetic Resonance* (Harper and Row, New York, 1963), p. 43.

[27]R. T. Schumacher and C. P. Slichter, Phys. Rev. 101, 58 (1956); R. T. Schumacher and W. E. Vehse, J. Phys. Chem. Solids 24, 297 (1963).

[28]C. Ryter, Phys. Rev. Letters 5, 10 (1960).

[29]M. Gueron, Phys. Rev. 135, A200 (1964).

[30]W. D. Knight, in *Solid State Physics*, edited by

F. Seitz and D. Turnbull (Academic, New York, 1956), Vol. 2.
[31]E. T. Micah, G. M. Storks, and W. H. Young, J. Phys. C 2, 1653 (1969).
[32]D. Pines, in *Solid State Physics*, edited by F. Seitz and D. Turnbull (Academic, New York, 1955), Vol. 1.
[33]A. Abragam, *The Principles of Nuclear Magnetism* (Clarendon, Oxford, 1961), p. 273.
[34]Reference 33, p. 314.
[35]W. W. Warren, Jr. and W. G. Clark, Phys. Rev. 177, 600 (1969); 184, 606 (1969).
[36]J. Korringa, Physica 16, 601 (1950).
[37]A. Narath and H. T. Weaver, Phys. Rev. 175, 373 (1968).
[38]R. W. Shaw, Jr. and W. W. Warren, Jr., Phys. Rev. B 3, 1562 (1971).
[39]F. A. Rossini and W. D. Knight, Phys. Rev. 178, 641 (1969).
[40]Reference 24, p. 116.
[41]See, for example, Ref. 33, Chap. VIII for a discussion of quadrupolar relaxation via rotational modes; for diffusional relaxation, see C. A. Sholl, Proc. Phys. Soc. (London) 91, 130 (1967).
[42]V. M. Glazov, S. N. Chizhevskaya, and N. N. Glagoleva, *Liquid Semiconductors* (Plenum, New York, 1969).
[43]Materials Research Corp., Orangeburg, N. Y.
[44]Reference 33, p. 292.
[45]R. P. Elliot, *Constitution of Binary Alloys, First Supplement* (McGraw-Hill, New York, 1965).
[46]A. I. Zaslavski and V. M. Sergeeva, Fiz. Tverd. Tela 2, 2872 (1960) [Sov. Phys. Solid State 2, 2556 (1961)].
[47]P. J. Holmes, I. C. Jennings, and J. E. Parrott, J. Phys. Chem. Solids 23, 1 (1962).
[48]P. E. Newman and J. A. Cundall, Nature 200, 876 (1963).
[49]V. P. Zhuze and A. I. Shelykh, Fiz. Tverd. Tela 7, 2430 (1965)[Sov. Phys. Solid State 7, 942 (1965)].
[50]J. R. Drabble and C. H. L. Goodman, J. Phys. Chem. Solids 5, 142 (1958).
[51]J. Black, E. M. Conwell, L. Seigle, and C. W. Spencer, J. Phys. Chem. Solids 2, 240 (1957).
[52]W. D. Knight, R. R. Hewitt, and M. Pomerantz, Phys. Rev. 104, 271 (1956).
[53]H. G. Dehmelt, Phys. Rev. 92, 1240 (1953).
[54]R. Blakeway, Phil. Mag. 20, 965 (1969).
[55]M. D. Banus, R. E. Hanneman, M. Strongin, and K. Gooen, Science 192, 662 (1963).
[56]K. C. Brog, W. H. Jones, Jr., and F. J. Milford, Phys. Rev. 144, 245 (1966).
[57]The choice of one s electron per Ga ion is based on the assumption that the bonding in "metallic" Ga_2Te_3 should have a high degree of ionicity as in InTe II (Ref. 56). In this case the configuration of the Ga ion is approximately $Ga^{++}(4s^1)$. However, because of the cube-root dependence of the free-electron density of states on the electron concentration, the estimated values of g are not highly sensitive to this assumption.
[58]L. S. Palatnik, L. V. Atroshchenko, L. P. Gol'chinetskii, and V. M. Koshkin, Dokl. Akad. Nauk. SSSR 165, 539 (1965) [Sov. Phys. Doklady 10, 1215 (1966)].
[59]M. H. Cohen, J. Non-Cryst. Solids 4, 391 (1970).
[60]T. E. Faber and J. M. Ziman, Phil. Mag. 11, 153 (1965).

PHYSICAL REVIEW B VOLUME 3, NUMBER 11 1 JUNE 1971

Doppler-Shifted Ultrasonic Spin Resonance in Metals*

Harold N. Spector
Physics Department, Illinois Institute of Technology, Chicago, Illinois 60616

and

J. B. Ketterson
Argonne National Laboratory, Argonne, Illinois 60439
(Received 11 December 1970)

A new method of measuring the conduction-electron g factor by ultrasonic Doppler-shifted spin resonance is presented. A Boltzmann-equation approach is used to obtain the attenuation arising from both the self-consistent-field and the Yafet mechanisms. The magnitude of the spin-dependent part of the attenuation is too small at the usual ultrasonic frequencies to be observed directly but the derivative of the attenuation should be observable.

I. INTRODUCTION

There now exist well-developed experimental techniques such as the de Haas–van Alphen (dHvA) effect, ultrasonic geometric resonance, microwave cyclotron resonance, etc., by which the shape of the Fermi surface and the Fermi velocity may be explored. Another interesting physical quantity associated with conduction electrons is their g factor. If the g factor is isotropic, the conduction-electron spin-resonance (CESR) technique may be used.[1] If the g factor is anisotropic, this technique is less useful, and other experimental techniques should be explored. The harmonic content of the amplitude of the dHvA oscillations contains information on the g factor associated with extremal orbits, but precise